Electrolytically Generated Nanobubbles on Highly Orientated Pyrolytic Graphite Surfaces

Shangjiong Yang,[†,‡] Peichun Tsai,[†] E. Stefan Kooij,[‡] Andrea Prosperetti,[†,§] Harold J. W. Zandvliet,[‡] and Detlef Lohse*[,†]

Physics of Fluids and Solid State Physics Groups, Faculty of Science and Technology, MESA+ Institute for Nanotechnology, University of Twente, 7500AE Enschede, The Netherlands, and Department of Mechanical Engineering, Johns Hopkins University, Baltimore, Maryland 21218

Received August 22, 2008. Revised Manuscript Received October 5, 2008

Electrolysis of water is employed to produce surface nanobubbles on highly orientated pyrolytic graphite (HOPG) surfaces. Hydrogen (oxygen) nanobubbles are formed when the HOPG surface acts as a negative (positive) electrode. The coverage and volume of the nanobubbles increase with increasing voltage. The yield of hydrogen nanobubbles is much larger than the yield of oxygen nanobubbles. The growth of the individual nanobubbles during the electrolysis process is recorded in time with the help of AFM measurements and correlated with the total current. Both the size of the individual nanobubbles and the total current saturate typically after 1 min; then the nanobubbles are in a dynamic equilibrium, meaning that they do not further grow, in spite of ongoing gas production and nonzero current. The surface area of nanobubbles shows a good correlation with the nanobubble volume growth rate, suggesting that either the electrolytic gas emerges directly at the nanobubbles' surface or it emerges at the electrode's surface and then diffuses through the nanobubbles' surface. Moreover, the experiments reveal that the time constants of the current and the aspect ratio of nanobubbles are the same under all conditions. Replacement of pure water by water containing a small amount of sodium chloride (0.01 M) allows for larger currents, but qualitatively gives the same results.

Introduction

Nanobubbles, nanoscopic gas bubbles present at solid−liquid interfaces,[1−16] are in many ways fascinating objects in the field of surface science and nanofluidics. It has been conjectured that they are relevant for a number of phenomena and technical applications, e.g., the liquid slippage at walls,[14,17−20] the stability of colloidal systems,[21] and the nanometer-scale attractive force between hydrophobic surfaces in solutions.[2,3,22−26] Studies on various physical aspects of nanobubbles have been increasingly undertaken in the past few years.[3,5−13,27−31] The solid surfaces employed in these studies include gold,[6] polystyrene,[8,9,11] mica,[28] silane-hydrophobilized silicon wafers,[5,12,29,30] and highly orientated pyrolytic graphite (HOPG).[10,12,13] Most studies are done with highly purified water (Milli-Q), though some experiments

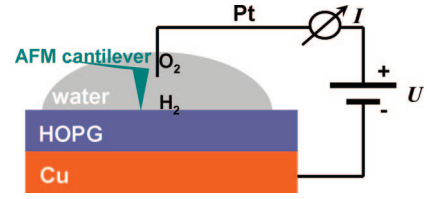

Figure 1. Sketch describing our experimental setup. The HOPG sample is placed on a copper plate. A platinum wire of diameter 0.25 mm is set (∼2 mm away) next to the AFM cantilever. The copper plate and the platinum wire are connected to a power source supplying the voltage *U* (the electrometer). The platinum wire and the HOPG surface act as the electrodes. The current *I* is measured with a high-precision amperemeter. When the HOPG surface is used as the negative (positive) electrode, a water reduction (oxidation) process takes place, producing hydrogen (oxygen) molecules on the HOPG surface.

* Corresponding author. E-mail: d.lohse@utwente.nl.
† Physics of Fluids Group, University of Twente.
‡ Solid State Physics Group, University of Twente.
§ Johns Hopkins University.

(1) Ball, P. *Nature* **2003**, *423*, 25.
(2) Vinogradova, O. I.; Bunkin, N. F.; Churaev, N. V.; Kiseleva, O. A.; Lobeyev, A. V.; Ninham, B. W. *J. Colloid Interface Sci.* **1995**, *173*, 443.
(3) Tyrrell, J. W. G.; Attard, P. *Phys. Rev. Lett.* **2001**, *87*, 176104.
(4) Attard, P. *Adv. Colloid Interface Sci.* **2003**, *104*, 75.
(5) Yang, S.; Dammer, S. M.; Bremond, N.; Zandvliet, H. J. W.; Kooij, E. S.; Lohse, D. *Langmuir* **2007**, *23*, 7072.
(6) Holmberg, M.; Kühle, A.; Garnæs, J.; Mørch, K. A.; Boisen, A. *Langmuir* **2003**, *19*, 10510.
(7) Borkent, B. M.; Dammer, S. M.; Schönherr, H.; Vancso, G. J.; Lohse, D. *Phys. Rev. Lett.* **2007**, *98*, 204502.
(8) Simonsen, A. C.; Hansen, P. L.; Klösgen, B. *J. Colloid Interface Sci.* **2004**, *273*, 291.
(9) Vinogradova, O. I.; Yakubov, G. E.; Butt, H. J. *J. Chem. Phys.* **2001**, *114*, 8124.
(10) Yang, S.; Kooij, E. S.; Poelsema, B.; Lohse, D.; Zandvliet, H. J. W. *Europhys. Lett.* **2008**, *81*, 64006.
(11) Agrawal, A.; Park, J.; Ryu, D. Y.; Hammond, P. T.; Russel, T. P.; McKinley, G. H. *Nano Lett.* **2005**, *5*, 1751.
(12) Zhang, X. H.; Maeda, N.; Craig, V. S. J. *Langmuir* **2006**, *22*, 5025.
(13) Zhang, L.; Zhang, Y.; Zhang, X.; Li, Z.; Shen, G.; Ye, M.; Fan, C.; Fang, H.; Hu, J. *Langmuir* **2006**, *22*, 8109.
(14) Neto, C.; Evans, D. R.; Bonaccurso, E.; Butt, H. J.; Craig, V. S. J. *Rep. Prog. Phys.* **2005**, *68*, 2859.
(15) Zhang, X. H.; Quinn, A.; Ducker, W. A. *Langmuir* **2008**, *24*, 4756.
(16) Zhang, X. H.; Khan, A.; Ducker, W. A. *Phys. Rev. Lett.* **2006**, *98*, 136101.
(17) Lauga, E.; Brenner, M. P.; Stone, H. A. In *Handbook of Experimental Fluid Dynamics*; Tropea, C., Foss, J., Yarin A., Eds.; Springer: New York, 2005.
(18) Vinogradova, O. I. *Langmuir* **1995**, *11*, 2213.
(19) Bunkin, N. F.; Kiseleva, O. A.; Lobeyev, A. V.; Movchan, T. G.; Ninham, B. W.; Vinogradova, O. I. *Langmuir* **1997**, *13*, 3024.
(20) de Gennes, P. G. *Langmuir* **2002**, *18*, 3413.
(21) Nguyen, A. V.; Evans, G. M.; Nalaskowski, J.; Miller, J. D. *Exp. Therm. Fluid Sci.* **2004**, *28*, 387.
(22) Parker, J. L.; Claesson, P. M.; Attard, P. *J. Phys. Chem.* **1994**, *98*, 8468.
(23) Attard, P. *Langmuir* **1996**, *12*, 1693.
(24) Tyrrell, J. W. G.; Attard, P. *Langmuir* **2002**, *18*, 160.
(25) Considine, R. F.; Hayes, R. A.; Horn, R. G. *Langmuir* **1999**, *15*, 1657.
(26) Yakubov, G. E.; Butt, H. J.; Vinogradova, O. I. *J. Phys. Chem. B* **2000**, *104*, 3407.
(27) Ishida, N.; Inoue, T.; Miyahara, M.; Higoashitani, K. *Langmuir* **2000**, *16*, 6377.
(28) Zhang, X. H.; Zhang, X. D.; Lou, S. T.; Zhang, Z. X.; Sun, J. L.; Hu, J. *Langmuir* **2004**, *20*, 3813.
(29) Agrawal, A.; McKinley, G. H. *Mater. Res. Soc. Symp. Proc.* **2006**, 899E.
(30) Switkes, M.; Ruberti, J. W. *Appl. Phys. Lett.* **2004**, *84*, 4759.
(31) Steitz, R.; Gutberlet, T.; Hauss, T.; Klösgen, B.; Krastev, R.; Schemmel, S.; Simonsen, A. C.; Findenegg, G. H. *Langmuir* **2003**, *19*, 2409.

10.1021/la8027513 CCC: $40.75 © 2009 American Chemical Society
Published on Web 01/05/2009

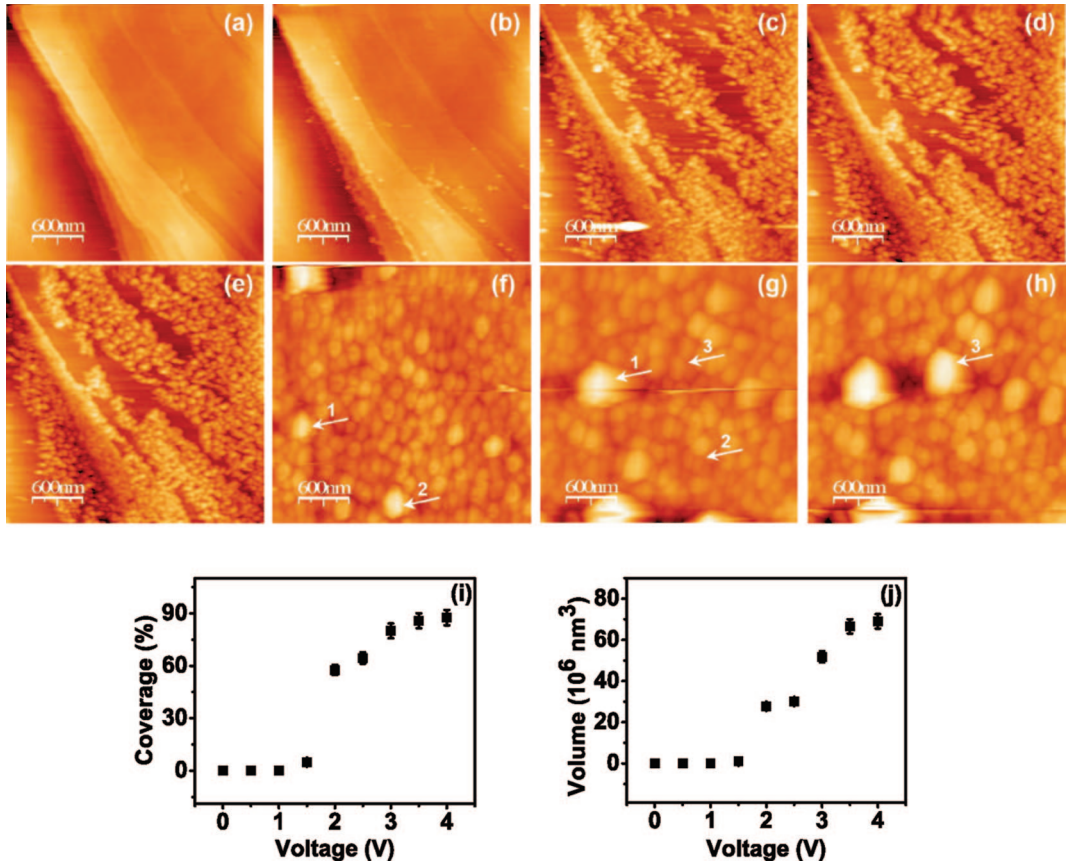

Figure 2. AFM (tapping mode) topography images of the HOPG surface (under water) as the cathode at different voltages: (a) 1 V, (b) 1.5 V, (c) 2 V, (d) 2.5 V, (e) 0 V, (f) 3 V, (g) 3.5 V, and (h) 4 V. Height range: (a, b) 42 nm, (c−e) 50.6 nm, (f) 61.2 nm, (g, h) 115.5 nm. The scanning time per image is 8.5 min, and the images are taken in a sequence from (a) to (h). Hydrogen nanobubbles are produced on the surface. When the nanobubble coverage is low, the atomic steps traversing the HOPG surface are visible. The formation of nanobubbles increases tremendously when the voltage is increased from 1.5 to 2 V. In (e) the voltage has been switched off, while the nanobubbles remain stable. In (f)−(h), at higher voltages nanobubbles cover the entire surface with much larger individual sizes. Nanobubbles growing (marked by arrows 1 and 3) or detaching (marked by arrow 2) are observed. The dependence of the nanobubble coverage and volume on the applied voltage is shown as plots i and j (error bar ±5%), respectively. With increasing voltage, more hydrogen molecules are produced at the cathode (HOPG surface), enhancing the local gas concentration. This results in more and larger nanobubbles, as revealed by (i) and (j).

have been done with alcohol[8] or dilute sulfuric acid solution.[13] Atomic force microcopy (AFM) in tapping mode is adopted in most experiments,[3,5−8,10−13,27−29] while other techniques such as rapid cryofixation−freeze fracture,[30] neutron reflectometry,[31] high-energy X-ray reflectivity,[32] and internal reflection infrared spectroscopy[15] have also been employed. Experimental observations show that nanobubbles are very stable, having an extraordinary shape with a remarkably large aspect ratio[5,12] which even increases further with decreasing nanobubble size.[33] The lifetime of nanobubbles shows a dependence on the gas type.[15] Besides the surface hydrophobicity, the spatial dimensions of the hydrophobic domains on the surface are crucial for the formation of nanobubbles.[29] It has also been reported that the formation of nanobubbles is related to surface nanostructures: the majority of nanobubbles prefer to form in the vicinity of nanometer-deep grooves[5] or on the upper side of atomic steps[10] on the surfaces. In addition, an increase of the substrate temperature, water temperature, or gas concentration in water increases the density and size of nanobubbles.[5,28] These observations clearly reveal that the formation of nanobubbles is very sensitive to surface and liquid conditions. However, is there a simple method that leads to the controlled formation and growth of nanobubbles?

In electrochemical reactions, gas molecules are generated at electrode surfaces. Most studies have hitherto focused on miniature or micrometer-sized bubbles, which are formed at and subsequently detach from the electrodes; see refs 34−39 and references therein. The interest originates partly from the significant influence of the bubbles on reaction systems. For example, convection caused by the evolution of electrogenerated microbubbles increases electrolyte flow and can enhance production processes.[35] The interest in electrochemically generated nanobubbles is more recent. It has been hypothesized that the existence of nanobubbles at electrode surfaces favors the formation of submicrometer-sized vaterite tubes in electrolysis-induced mineralization.[36] Zhang et al.[13] confirmed that electrochemical generation of hydrogen induces the formation of nanobubbles on the electrode surface in sulfuric acid solution.

(32) Mezger, M.; Reichert, H.; Schöder, S.; Okasinski, J.; Schröder, H.; Dosch, H.; Palms, D.; Ralston, J.; Honkimäki, V. *Proc. Natl. Acad. Sci. U.S.A.* **2006**, *103*, 18401.
(33) Borkent, B. M.; Schönherr, H.; Lohse, D. To be submitted to *Phys. Rev. Lett.*
(34) Tsai, W. L.; Hsu, P. C.; Hwu, Y.; Chen, C. H.; Chang, L. W.; Je, J. H.; Lin, H. M.; Groso, A.; Margaritondo, G. *Nature* **2002**, *417*, 139.
(35) Boissonneau, P.; Byrne, P. *J. Appl. Electrochem.* **2000**, *30*, 767.
(36) Fan, Y.; Wang, R. *Adv. Mater.* **2005**, *17*, 2384.
(37) Volanschi, A.; Olthuis, W.; Bergveld, P. *Sens. Actuators, A* **1996**, *52*, 18.
(38) Gabrielli, C.; Huet, F.; Keddam, M.; Macias, A.; Sahar, A. *J. Appl. Electrochem.* **1989**, *19*, 617.
(39) Gabrielli, C.; Huet, F.; Keddam, M.; Sahar, A. *J. Appl. Electrochem.* **1989**, *19*, 683.
(40) Brenner, M. P.; Lohse, D. *Phys. Rev. Lett.* **2008**, *101*, 214505.

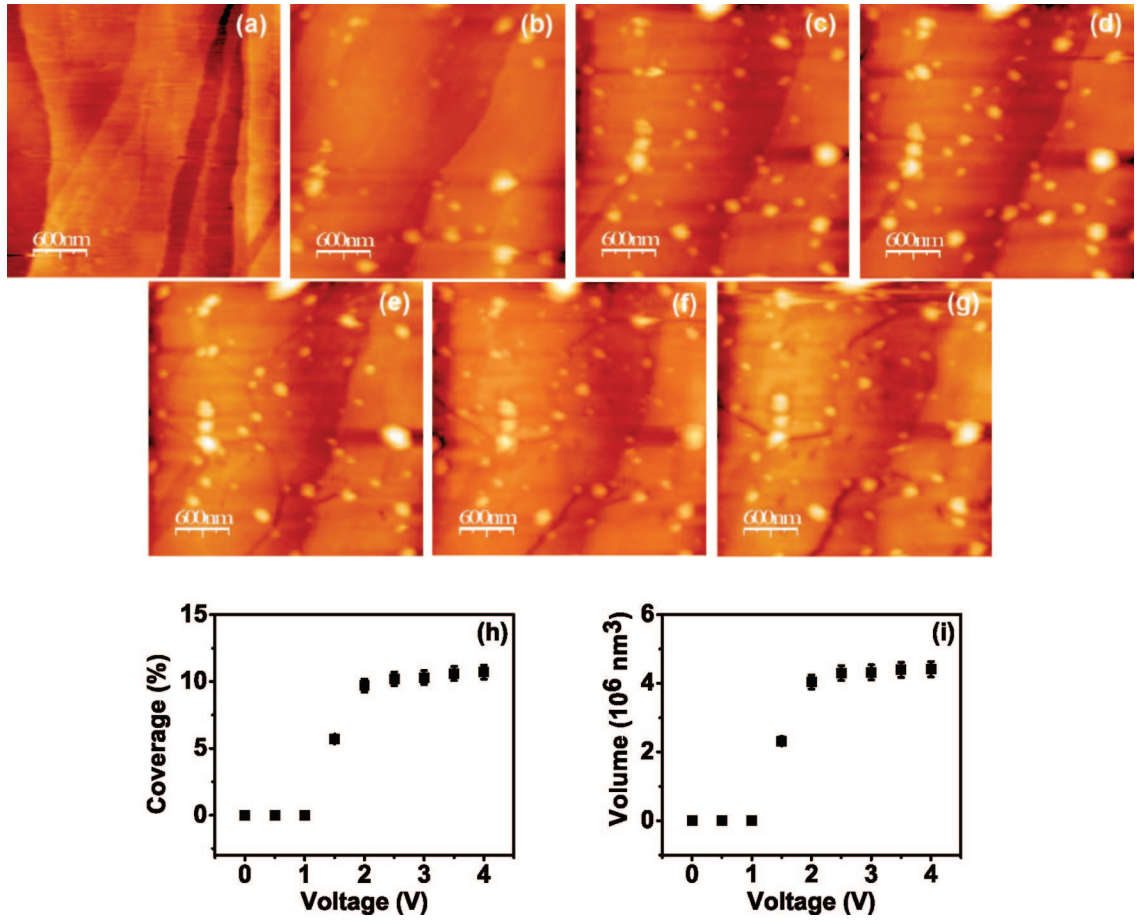

Figure 3. AFM (tapping mode) topography images of the HOPG surface (under water) as the anode at different voltages: (a) 1 V, (b) 1.5 V, (c) 2 V, (d) 2.5 V, (e) 3 V, (f) 3.5 V, and (g) 4 V. Height range: (a) 12 nm, (b−g) 35 nm. Again, the atomic steps of the HOPG surface are visible. Images are recorded continuously from (a) to (g), with a scanning time of 8.5 min per image. Nanobubbles (oxygen) are formed on the surface. Compared to the hydrogen case in Figure 2, the number and volume of the produced oxygen nanobubbles are much smaller. This is presumably due to (i) the considerable difference of solubility in water between oxygen and hydrogen (oxygen's solubility is ∼2 times higher than hydrogen's at 20 °C) and (ii) the difference in the production rate during electrolysis, H_2:O_2 = 2:1. (h) and (i) show the coverage and volume of the nanobubbles as a function of the imposed voltage, respectively (error bar ±5%).

The work described in this paper is motivated by two issues: (i) Electrolysis of water is a reliable and controllable way to rapidly produce a high local gas concentration at electrode surfaces. The gas concentration significantly affects the formation of nanobubbles.[5] Electrolysis of water therefore is an easy method to control the appearance and growth of surface nanobubbles. This is demonstrated in this study by performing AFM measurements of nanobubbles on an HOPG surface which acts as an electrode. To reduce the effect of any possible impurities in the liquid, since nanobubbles are extremely sensitive to surfactants, ultraclean water (see below for qualification) is used as the electrolyte. In addition, to test the reproducibility, an aqueous sodium chloride solution (0.01 M) is also used. We study the bubble coverage, volume, size, and aspect ratio at different voltages. In addition, we show the real-time development of individual nanobubbles, before they finally achieve a dynamic equilibrium condition. Remarkably, the nanobubble's surface area and its volume growth are highly correlated, suggesting that either the electrolytic gas is produced at the whole surface of the nanobubbles, or it is generated at the electrode's surface and diffuses to the surface of the nanobubbles. (ii) The second issue of this paper is to correlate the geometric feature of the nanobubbles with the electric current that flows between the two electrodes. We find a good correlation between the aspect ratio of the nanobubbles and the current.

Experimental Section

The water is prepared by a Milli-Q Synthesis A10 system (Millipore SAS, France) and then degassed at 1 mbar for 4 h. AFM measurements are done with a PicoSPM (Molecular Imaging, Arizona) operated in tapping mode. Excitation of the tip vibration is done acoustically, using a small piezoelement in the tip holder. The AFM operating parameters in water are as follows: scanning speed 6 μm/s, free amplitude 400 mV, set-point amplitude 300 mV, resonance frequency 20 kHz. AFM scanning is performed by a hydrophilic Si_3N_4 ultrasharp AFM tip (radius of curvature <10 nm, full tip cone angle <30°, NSC18/AlBS, MikroMasch, France, rinsed with ethanol and pure water before use). An HOPG sample (HOPG ZYB/1.75, size 10 mm × 10 mm, MikroMasch, France) with a freshly cleaved surface placed on a copper plate is used as a nanobubble-forming surface and at the same time as one of the electrodes. A platinum wire (diameter 0.25 mm) placed next to the AFM cantilever is used as the other electrode. The copper plate and the platinum wire are connected to an electrometer (Picoammeter/Voltage Source 6478, Keithley Instruments Inc., Ohio). After a water drop (volume 0.33−0.40 mL) is placed on the HOPG surface and the desired voltage is imposed, the AFM scanning process is started immediately. Figure 1 shows a sketch of the setup. When the HOPG sample acts as the negative electrode (cathode), the reduction process of water leads to the formation of hydrogen molecules on the HOPG surface, $2H_2O(l) + 2e^- \rightarrow H_2(g) + 2OH^-(aq)$. Oxygen molecules are produced on the HOPG surface when the HOPG sample is switched to be the positive electrode (anode), and therefore the

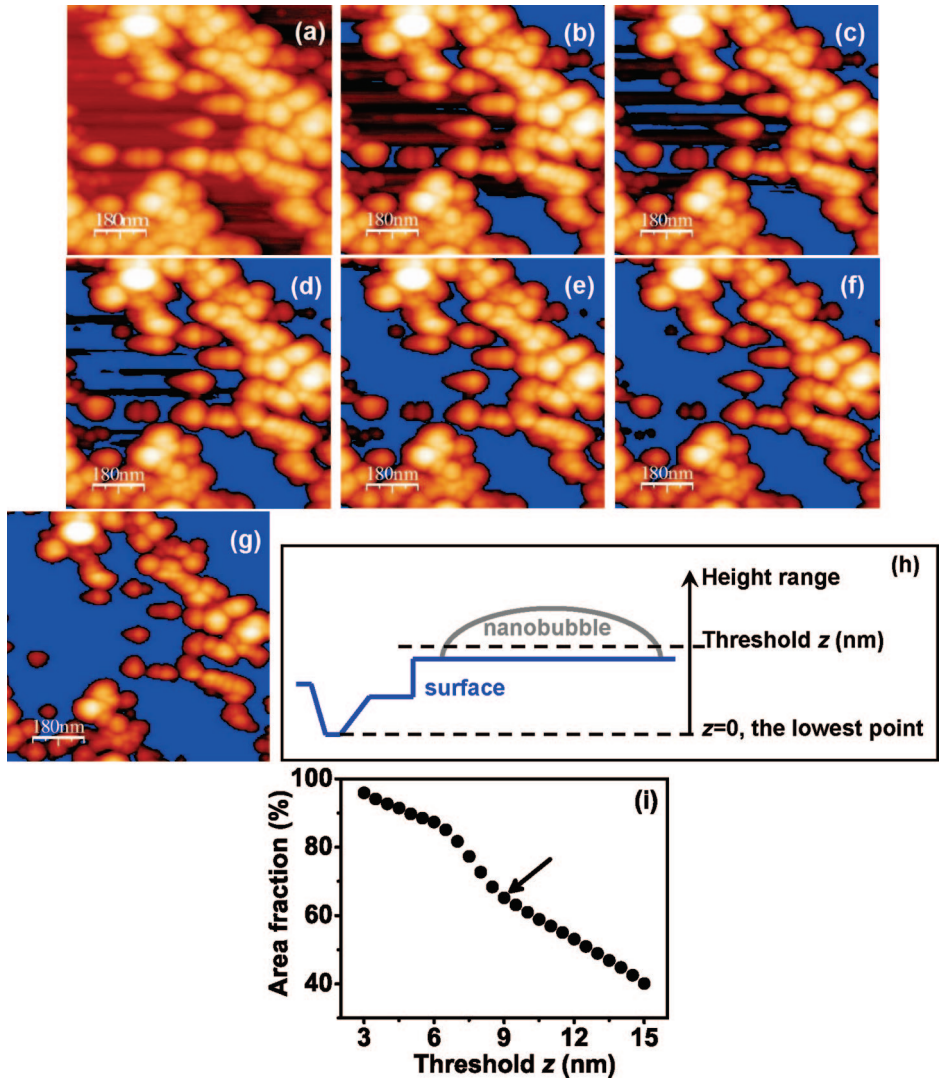

Figure 4. Tapping mode AFM topography images (height range 27.2 nm) of hydrogen surface nanobubbles when different thresholds z are applied for the identification of surface nanobubbles: (a) $z = 0$ nm, (b) $z = 6$ nm, (c) $z = 7$ nm, (d) $z = 8$ nm, (e) $z = 9$ nm, (f) $z = 10$ nm, and (g) $z = 14$ nm. Sketch h describes the principle. Areas below this threshold are given as blue and areas above, depending on the height, as yellow. The fraction of the latter area is shown in (i) as a function of the threshold z. That curve shows a pronounced shape. We take the end of the straight shape region (see the arrow and $z = 9$ nm) toward smaller z as an estimate for the nanobubble coverage.

oxidation process of water on the surface leads to oxygen molecules, $2H_2O(l) \rightarrow O_2(g) + 4e^- + 4H^+(aq)$. The experiments are carried out in a standard laboratory environment with a temperature between 20 and 23 °C. The temperature change of the HOPG sample during the measurements is less than 0.1 K.

Results and Discussion

Nanobubbles by Electrolysis of Water: Dependence on the Applied Voltage and Gas Type. Previous experimental results show that no nanobubbles are formed on HOPG surfaces unless the so-called ethanol−water exchange step is carried out.[10,12] This is due to the hydrophilic nature of the surface (macroscopic contact angle <90°) that disfavors the attachment of surface bubbles. Electrolysis of water can be a robust method for a sufficient yield of nanobubbles on HOPG.[13] AFM measurements by tapping mode are performed on the HOPG surface.

Figure 2 shows the topography images of the HOPG surface used as the cathode with different applied voltages: (a) 1 V, (b) 1.5 V, (c) 2 V, (d) 2.5 V, (e) 0 V, (f) 3 V, (g) 3.5 V, (h) 4 V. The height range for each image is (a, b) 42 nm, (c−e) 50.6 nm, (f) 61.2 nm, and (g, h) 115.5 nm. The images are recorded continuously from (a) to (h), with a scanning time of 8.5 min per image. Nanobubbles (hydrogen) form with varying density at different voltages. The atomic steps of HOPG are visible when the nanobubble coverage is low and thus act as a good reference position at the nanoscale when AFM measurements are conducted. The formation of nanobubbles increases tremendously when the voltage is increased from 1.5 to 2 V. Figure 2e reveals that the nanobubbles remain stable even when the voltage has been switched off from 2.5 V (d). This demonstrates the robust stability of nanobubbles, which is similar to the previous finding that the heating-water-generated nanobubbles do not disappear when the water is cooled.[5] At the higher voltages, nanobubbles cover the entire surface with much larger individual sizes; see Figure 2f−h. Growth and detachment of nanobubbles are observed under the higher electric potentials; the examples are marked by arrows in the images. The dependence of the nanobubble coverage and volume on the applied voltage is respectively depicted in parts i and j of Figure 2 (error bar ±5%). With increasing voltage, more hydrogen molecules are produced at the cathode (HOPG surface), enhancing the local gas concentration. This leads to an increase in the coverage and volume of the nanobubbles, as revealed by plots i and j in Figure 2. At high voltages, i.e., 4.5

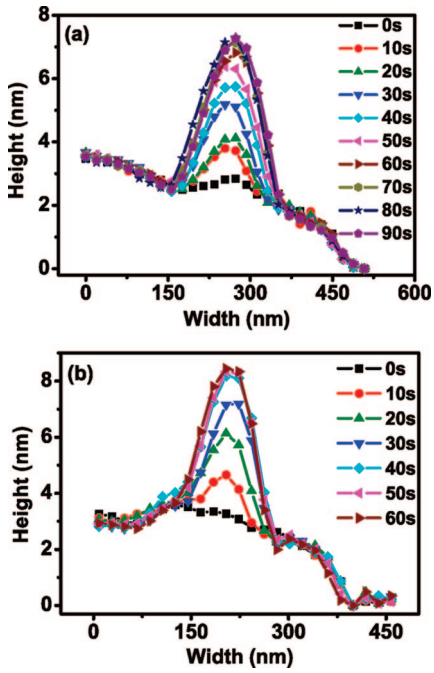

Figure 5. (a) Real-time profiles of a nanobubble on an HOPG surface (as the cathode) at 1 V with a time interval of 10 s. Another example at 2 V is shown in (b). By means of electrolysis of water, nanobubbles form on the surface and subsequently grow. In (a) the growth terminates after 70 s, while in (b) this occurs already after 40 s. The nanobubbles then remain stable. The plots also reveal that the nanobubbles grow with a higher rate in height rather than in width.

or 5 V, microbubbles developing at the HOPG surface can already be monitored by an optical camera. The evolution of these microbubbles ruins the AFM scanning process by interfering with the vibrating AFM cantilever.

AFM topography images of the HOPG surface used as the anode are shown in Figure 3. Different voltages are applied: (a) 1 V, (b) 1.5 V, (c) 2 V, (d) 2.5 V, (e) 3 V, (f) 3.5 V, (g) 4 V. The height range for each image is (a) 12 nm and (b−g) 35 nm. The scanning time of each image is 8.5 min. The images are taken in succession from (a) to (g) without any delay. Oxygen nanobubbles form on the surface. Compared to the hydrogen case in Figure 2, the production of nanobubbles in Figure 3 is much smaller. We suggest that this is due to the considerable difference in the solubility of oxygen and hydrogen in water (at 20 °C the solubility of oxygen is ∼2 times higher than that of hydrogen), as well as to the different production rates during electrolysis, H_2:O_2 = 2:1. The nanobubble coverage and volume are plotted as functions of the applied voltage, respectively, in parts h and i of Figure 3 (error bar ±5%). For both hydrogen and oxygen, the plots in Figures 2i,j and 3h,i reveal a threshold and saturation of the nanobubble formation dependent on the applied voltage.

The coverage and volume values presented in Figures 2i,j and 3h,i are calculated by setting an appropriate height threshold z to extract nanobubbles. This is illustrated by the example in Figure 4. AFM (tapping mode) topography images (height range 27.2 nm) of hydrogen surface nanobubbles are shown with different thresholds z applied for the identification of surface nanobubbles: (a) $z = 0$ nm, (b) $z = 6$ nm, (c) $z = 7$ nm, (d) $z = 8$ nm, (e) $z = 9$ nm, (f) $z = 10$ nm, and (g) $z = 14$ nm. The principle is sketched in Figure 4h. Areas below the threshold are represented in blue, whereas areas above are shown as yellow depending on the height. The fraction of the latter area is shown in Figure 4i as a function of the threshold z. The curve shows a pronounced shape. We take the value at the end of the straight shape region (marked by an arrow), where $z = 9$ nm presents a nanobubble identification as shown in image e, as an estimate for the nanobubble coverage and volume statistics.

Nanobubbles in Dynamic Equilibrium. During the experiments, each chosen voltage is continuously applied while the AFM measurements shown in Figures 2 and 3 are performed. The constant voltage results in continuous charge flux through the system. Under such a condition, one may expect that surface nanobubbles would constantly accumulate on the electrode surfaces. However, our AFM images (Figures 2 and 3), taken after a certain transient time, show stationary nanobubbles of

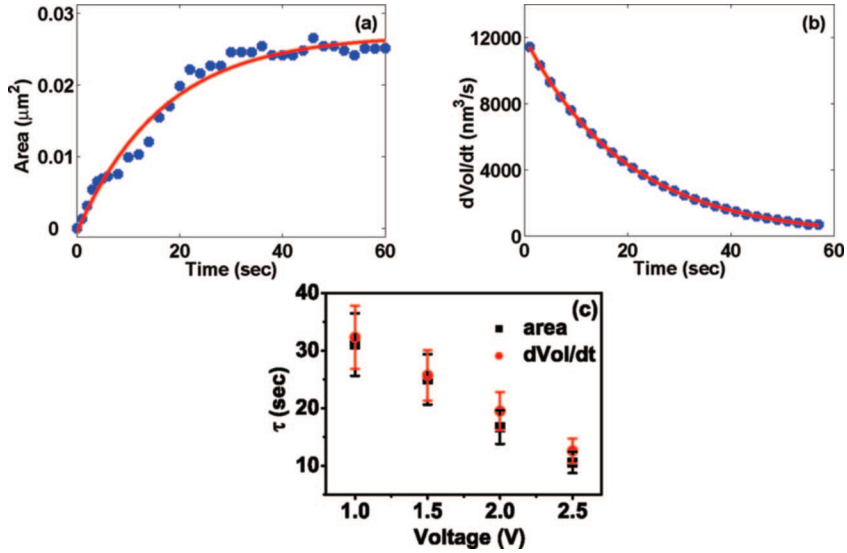

Figure 6. Nanobubble area (a) and volume growth rate (b) plots (blue dots). The red curves are fits of an exponential function, $X = X_\infty + (X_0 - X_\infty)e^{-t/\tau}$, where X is either the area or the volume growth rate. These fits allow definition of a characteristic time scale, τ. Values of the time constant τ extracted from the fits are exhibited as a function of the applied voltage, as shown in (c). The time scales of the area evolution (black squares) and the volume growth rate evolution (red dots) show a good correlation at all voltages. This observation suggests two possible ways of how the electrolytic gas is produced on the surface: (i) the gas emerges at the whole surface of the nanobubbles, and correspondingly, the whole surface of the nanobubbles should be charged by electrons; (ii) the gas emerges at the electrode surface and then diffuses through the nanobubble surface.

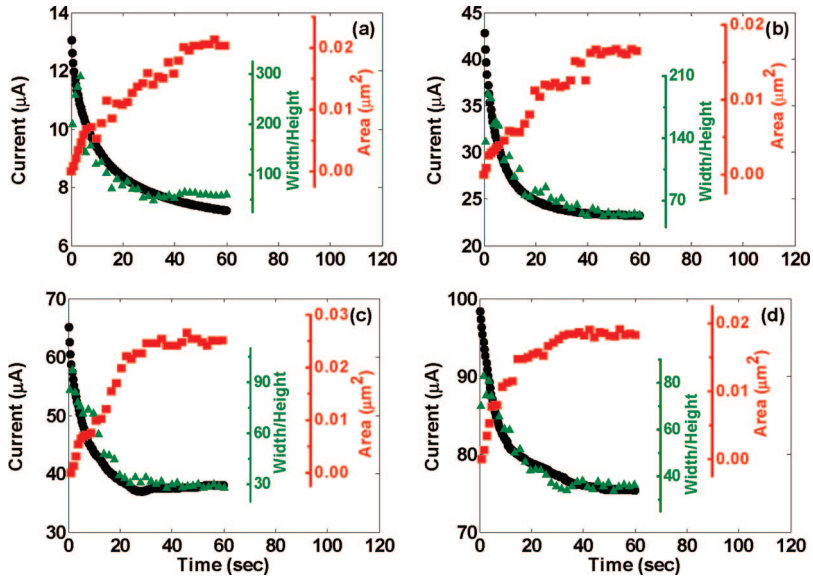

Figure 7. Graphs showing the current, nanobubble area, and nanobubble aspect ratio (width/height) as a function of time at (a) 1 V, (b) 1.5 V, (c) 2 V, and (d) 2.5 V on HOPG as the cathode. At each voltage, the three plots are recorded simultaneously. Nanobubble development and the current decay show a clear correlation. Interestingly, the current and the nanobubble aspect ratio (green triangles) decrease in the same manner. The aspect ratio plot indicates that nanobubbles initially form in an ultrathin film form and then accumulate with a higher rate in the vertical direction rather than in the horizontal direction; this is consistent with the findings shown in Figure 5.

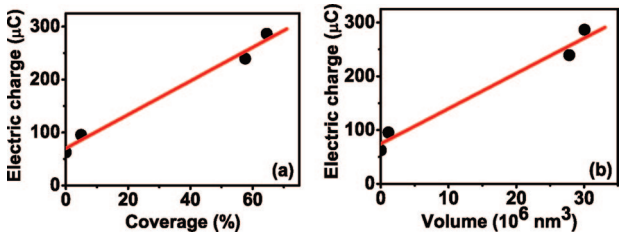

Figure 8. Amount of excess electric charge above the equilibrium (within 60 s) is estimated for each voltage, namely, 1, 1.5, 2, and 2.5 V. It is plotted versus the nanobubble coverage (a) and the volume (b). The red lines are linear fits. Note the offset of the linear fits: A finite amount of charge is needed before nanobubbles are produced, presumably to build up dielectric layers at the interface.

certain sizes. In other words, electrolytically generated nanobubbles experience a saturation in their development.

This suggests that the nanobubbles are in a *dynamic equilibrium* state. There are gas flows into and out of the nanobubbles simultaneously which balance each other, allowing for a constant volume. When the inflow overwhelms the outflow, nanobubbles start to grow. This happens when the voltage is increased, producing more charges and leading to a larger gas flow into the nanobubbles, thus breaking the previous balance between the inflow and the outflow, and consequently causing the nanobubbles to grow. As the nanobubbles grow, the outflow starts to increase till it reaches a new equilibrium state with the inflow. The nanobubbles then again remain in a stable condition.

To quantify the growing process of the nanobubbles, we focus on a number of individual nanobubbles and measure the evolution of various geometric properties such as width, height, aspect ratio, etc. In addition and in parallel, we measure the global current as a function of time (shown in the following sections). The electric current decays as the nanobubbles grow. This decrease in current, which reduces the amount of gas produced on the surface, effectively decreases the inflow to the nanobubbles. This of course helps to reach a new dynamic equilibrium state, but we stress again that the current is nonzero in the saturated state. The data of the current as a function of time and the nanobubble development show saturation on the same time scale. At the saturated state, the nanobubble growth terminates, whereas the saturated current is nonzero. This observation clearly suggests the existence of a *dynamic equilibrium* of the nanobubbles.

Time Evolution of Nanobubbles. The appearance of nanobubbles can easily be controlled by an increase of the voltage, as revealed in Figures 2 and 3. Thus, we can capture the dynamics of nanobubble growth by operating the AFM tip to repeatedly scan along a fixed straight line on the surface over the time of the electrolysis. With this method we perspicuously quantify the evolution of the nanobubbles at the moment of increasing voltage. The measurements are shown in Figure 5.

During the experiment, we first start the AFM scan over one line on the HOPG surface, and then we apply the desired voltage to generate surface nanobubbles. Meanwhile the AFM scan is continuously running. The time when we apply the voltage is taken as 0. Each AFM line scan takes 1 s; the profile of the developing nanobubble is continuously recorded. Figure 5a presents the profiles of a nanobubble generated with 1 V and the adjacent substrate surface (HOPG, as the cathode) at different times with an interval of 10 s. Plot b exhibits the dynamics of another nanobubble generated at 2 V. It is clearly shown that the nanobubbles start to grow continuously immediately after their appearance on the surface; this is also demonstrated by the nanobubble area vs time plots in Figures 6 and 7. Note that the growth terminates after 70 s for plot a and after 40 s for plot b in Figure 5. The nanobubbles then remain stable, although the voltage is still applied and the current is nonzero. The stabilized nanobubble in Figure 5a is approximately 200 nm in width and 5 nm in height. Interestingly, the measurements show that the nanobubbles grow with a faster rate in height than in width. The good agreement in the topography among the profiles of the adjacent HOPG surfaces at different times reveals that the AFM measurement is not considerably perturbed by the electrolysis process or the emergence of the nanobubbles. The profiles of the nanobubble therefore can be compared.

From the nanobubble profiles recorded by the AFM scan, we extract the width and height values of the nanobubbles at different times. Note that the AFM scan does not necessarily cross the

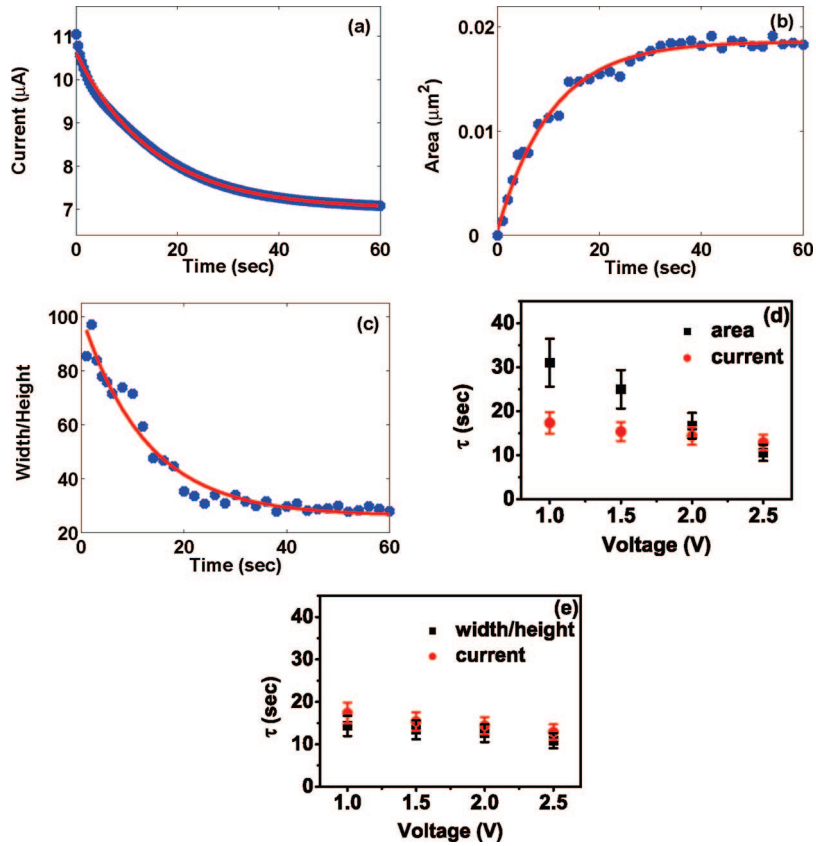

Figure 9. Exponential fits (red curves) of the current (a), nanobubble area (b), and nanobubble aspect ratio (width/height) (c) plots (blue dots). Values of the time constant τ of the fits are extracted. τ is plotted versus the voltage for the area (error bar $\pm$17%) and current (error bar $\pm$13%) as shown in (d), as well as for the width/height (error bar $\pm$16%) and current as shown in (e). τ decreases with increasing voltage; this indicates that the development of nanobubbles and the decay of the current take place more rapidly at higher voltage. The τ values of the area and the current well agree at 2 and 2.5 V when the nanobubble coverage is high. At 1 and 1.5 V, when the nanobubble coverage is rather low, the time constants of the area and current deviate. Note that the current is a global measure, whereas the area of individual nanobubbles is a local quantity. Interestingly, the nanobubble aspect ratio and the current always show good agreement (e), for which we do not have proper explanations.

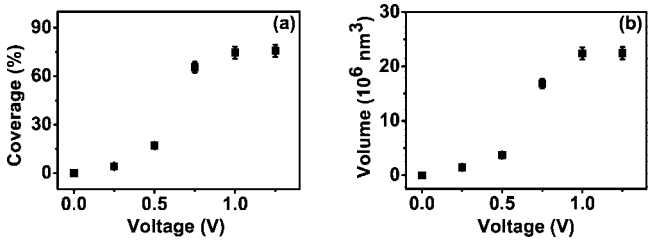

Figure 10. Sodium chloride (NaCl) solution (0.01 M) is used instead of pure water as the electrolyte. Behavior similar to that for pure water is observed: with increasing voltage the formation of hydrogen nanobubbles is enhanced (on HOPG as the cathode). The coverage and volume of the nanobubbles are related to the applied voltage, as depicted in (a) and (b) (error bar $\pm$5%), respectively. The required effective voltage for nanobubble creation is strongly reduced, as compared to the pure water case, as salty water has a lower resistance.

center (the maximum width and height) of each nanobubble. Therefore, the extracted width and height values may be lower than the maximum values. By assuming the shape of the nanobubbles as a spherical cap, we estimate the surface area of a nanobubble as $\pi w^2/4$ using the extracted width w. In a corresponding way we estimate the volume growth rate of a nanobubble, which as well as the surface area is then plotted as a function of time, shown in parts a and b, respectively, of Figure 6. Exponential fits (red lines) are applied to both plots, and values of the time constant τ are extracted. τ values of the area and volume growth rate are plotted versus voltage in Figure 6c. The plot shows that the nanobubble area and volume growth rate have a good correlation at all four voltages. This result suggests that the electrolytically generated gas is produced on the whole surface of the nanobubbles, implying that the whole surface of the nanobubbles is electrically charged. Alternatively, the electrolytically generated gas could be produced on the electrode surface (HOPG) and subsequently diffuse through the surface of the nanobubbles.

Correlation between Global Current and Local Nanobubble Growth. The global current of the electrolysis system is recorded as a function of time with a sampling rate of 0.367 s and an integration time of 0.102 s. To test the reproducibility, two HOPG samples and three freshly cleaved surfaces on each sample are analyzed (as cathodes). Thus, current measurements are done on six different HOPG surfaces at each voltage. All these results show that the current vs time curves present an exponential decay at voltages below 3 V. At higher voltages, the current fluctuates strongly. The reason is that more and bigger bubbles are formed at higher voltages. Growth and detachment of the bubbles cause the current to fluctuate. This is in agreement with the observations in Figure 2 and refs 38 and 39.

As described in the previous section, we extract the width and height values of nanobubbles at different times, on the basis of the AFM-recorded profiles of the nanobubbles. We here estimate the nanobubble area and aspect ratio (width over height), which are then plotted as a function of time. In Figure 7, graphs show the dynamics of the current, nanobubble area, and nanobubble aspect ratio within the first 60 s at (a) 1 V, (b) 1.5 V, (c) 2 V, and (d) 2.5 V. These three quantities are recorded simultaneously

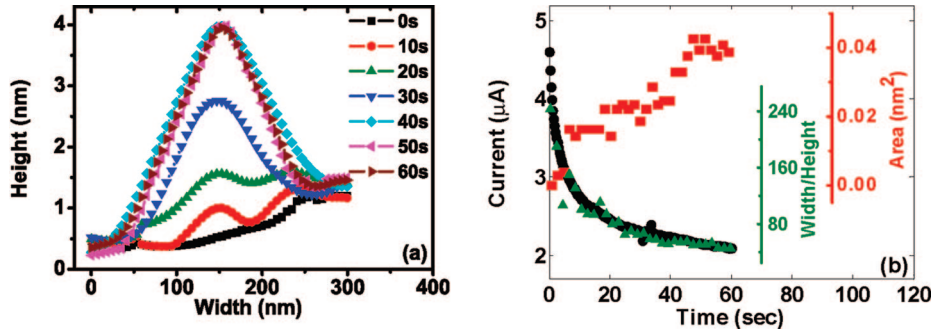

Figure 11. In the NaCl solution at 0.25 V, as analogous to Figures 5 and 7, (a) the time evolution of a hydrogen nanobubble is recorded. (b) The current, the nanobubble area, and the aspect ratio as a function of time are measured. Behaviors simlar to those for the pure water case are observed.

at each voltage. The nanobubble development and the current decay are strongly correlated. In Figure 7a, as an example, the nanobubble expands rapidly in the first 20 s, from 20 to 50 s it grows less quickly, and thereafter it reaches a stable state, as revealed by the area vs time plot (red squares); the current decay behaves in a correlated way on the same time scale (black dots). Interestingly, along with the current decay, the nanobubble aspect ratio (green triangles) decreases too. This indicates that nanobubbles occur initially in an ultrathin film form with a large aspect ratio and then accumulate with a higher growth rate in the vertical compared to the horizontal direction. This is consistent with the observation in Figure 5.

The gas produced at the electrode surface depends on the electric charge passing from one electrode to the other. Figure 7 shows that the global current reaches an equilibrium state as soon as the nanobubble development terminates. The amount of excess electric charge above the equilibrium state within 60 s is estimated for voltages of 1, 1.5, 2, and 2.5 V, respectively. The amount is plotted against the nanobubble coverage and volume at each voltage, as shown in parts a and b, respectively, of Figure 8. The red lines are linear fits. Note that the fits are guides to the eyes, not necessarily suggesting that both the coverage and volume of the nanobubbles have a linear relation with the charge. One can see that the amount of nanobubbles produced increases as the amount of excess electric charge increases, showing the contribution of the gas yielded by electrolysis to the nanobubble formation. Note the offset of the fits: in spite of the nonzero charge there is no nanobubble production (zero nanobubble coverage and volume). The offset indicates that part of the electrolytically generated gas dissolves, not contributing to the formation of nanobubbles. This crucial charge may also be needed to build up a dielectric layer at the electrode. Zhang et al. reported a similar observation that a formation time for nanobubbles is required and it decreases when the applied voltage increases.[13]

For further analysis of the time scales of the current and the nanobubble growth, the current, the nanobubble area, and the aspect ratio plots are fitted with an exponential. Examples are shown in Figure 9a−c. Red curves are the fits to the data (blue dots), from which the time constants τ are extracted. The values of τ are presented as a function of the voltage for the area (error ±17%) and current (error ±13%) in Figure 9d and for the aspect ratio (error ±16%) and current in Figure 9e. First, we note that the τ values decrease with increasing voltage, indicating that the development of nanobubbles and the decay of the current take place more rapidly at higher voltage. One can moreover see that the τ values of the area and current (i) agree well at 2 and 2.5 V when the nanobubble coverage is high (hence, the nanobubble growth leads to a decrease of the current in the system) and (ii) deviate at 1 and 1.5 V when the nanobubble coverage is rather low. We stress that the current is a global parameter, whereas the area of individual nanobubbles is a local parameter. Interestingly, the nanobubble aspect ratio and the current are perfectly correlated, as shown in Figures 7 and 9e. We do not have an explanation for this finding. We note that the aspect ratio presumably exhibits a universal way of nanobubble development. Therefore, it might be a global feature.

NaCl Solution as the Electrolyte. To study the robustness of our observations, in addition to pure water an aqueous sodium chloride (NaCl) solution (0.01 M) was used as the electrolyte. Using the same experimental setup as described in Figure 1, the NaCl solution is deposited on the HOPG surface acting as the negative electrode (cathode). With no applied voltage, no nanobubbles are formed. When the voltage is imposed, the formation of hydrogen nanobubbles starts to become observable. The voltage is varied as 0.25, 0.5, 0.75, 1, and 1.25 V. A small amount of nanobubbles are already formed at 0.25 V. The nanobubble formation increases tremendously as the voltage is switched from 0.5 to 0.75 V. This is similar to the result shown in Figure 2 where the formation of nanobubbles jumps from 1.5 to 2 V. The formation of nanobubbles in NaCl solution starts to show a saturation after 0.75 V. The dependence of the nanobubble coverage and volume on the applied voltage is depicted in parts a and b, respectively, of Figure 10 (error bar ±5%). When the voltage is higher than 1.25 V, AFM imaging is disturbed by bigger bubbles developing or detaching from the surface. The formation of nanobubbles in the NaCl solution is similar to that in pure water, except that because of the reduced resistance due to the dissolved salt, the effective voltage is reduced by a factor of about 3: 2 V for the pure water and 0.75 V for the NaCl solution. Note that the volume and coverage of nanobubbles at the effective voltages in the two cases are comparable.

The time evolution of nanobubbles at 0.25 V in the NaCl solution is shown in Figure 11. The nanobubbles continuously develop on the surface till 40 s and then remain stable, as revealed in Figure 11a. As in the experiment shown in Figure 7, the global current of the electrolysis system, the nanobubble surface area, and the aspect ratio are measured simultaneously as a function of time within the first 60 s, as shown in Figure 11b. A good correlation between the current decay and the nanobubble development is found; this is the same observation as with pure water. The aspect ratio also shows a comparable correlation with the current. The experiments with the NaCl solution reproduce our findings concerning the nanobubbles in dynamic equilibrium. Again, good correlations between the global current decay and bubble growth dynamics are found.

Conclusion

We have shown that the electrolysis of water is a reliable method to produce both hydrogen (at the cathode) and oxygen (at the anode) surface nanobubbles. The coverage and volume of the nanobubbles grow substantially with increasing voltage. The yield of hydrogen nanobubbles is much higher than that of oxygen nanobubbles. Our results of nanobubble evolution have shown that nanobubbles occur initially in an ultrathin film with a large aspect ratio, and subsequently grow with a higher rate in the vertical rather than the horizontal direction. In spite of the continuously applied voltage and a nonzero current, the growth of the nanobubbles terminates after a typical time, showing that electrolytically generated nanobubbles are in a dynamic equilibrium condition. We note that also the spontaneously forming nanobubbles (i.e., without electrolysis) might be in a dynamic equilibrium, in which the gas outflux through the Laplace pressure is compensated by a gas influx at the contact line, as has recently been speculated in ref 40. In addition, we have found a correlation between the surface area and the volume growth rate of nanobubbles, suggesting possible ways of how electrolytic gas emerges on the surface. The global current as a function of time is strongly correlated with the bubble aspect ratio. The experiments with an aqueous sodium chloride solution (0.01 M) give similar results.

Acknowledgment. We thank Bram Borkent, Michael Brenner, Bene Poelsema, and Jacco Snoeijer for stimulating discussions. This work is part of the research program of the Stichting voor Fundamenteel Onderzoek der Materie (FOM), financially supported by the Nederlandse Organisatie voor Wetenschappelijk Onderzoek (NWO).

LA8027513